# Gust load reduction concept in wind turbines

J. Grzędziński & A. Mróz
*Institute of Fundamental Technological Research, Polish Academy of Sciences, Warsaw, Poland*

ABSTRACT: A concept is presented of semi-active gust load alleviation in wind turbines. Blade aerodynamic torsional moment is used as an actuator for forcing the blade to feather and thus reducing aerodynamic loads. A simple wind turbine model is formulated in order to demonstrate that — at least theoretically — it is possible to change the blade pitch angle faster than with a regular pitch control actuator. The problem is formulated in generalized coordinates as well as using the modal method. A number of results of numerical simulation is also given.

## 1 INTRODUCTION

Despite all the knowledge about gust nature, actually each particular gust is unpredictable. Due to severe loading generated by wind gusts on a blade it would be very beneficial to have a certain mechanism in place, in order to react to a gust very quickly and avoid the wind turbine overloading. Such a mechanism should be simple, reliable, and also faster than the regular pitch control actuator. It should reduce gust generated aerodynamic forces and, consequently reduce the overall wind turbine loading.

For this purpose, in case of pitch controlled turbines, the aerodynamic torsional moment can be used, which twists the blade even in steady, normal operating conditions. A plot of the blade torsional moment $M_z$ as a function of wind speed $V_{wind}$ is shown in Figure 1. This particular plot corresponds to a pitch controlled, offshore, 5 MW described by (Lindenburg 2002). No pitch control is active until wind speed reaches 11 m/s. Above this speed, the control actuator is switched on and keeps the rotor torque $M_x$ constant, and so the rotor angular velocity. As can be seen, during the controlling process the blade torsional moment $M_z$ decreases as wind speed grows, and shortly reaches its negative values. A negative value of the torsional moment means that the pitch angle is forced to increase and if the rotational connection between a blade and a hub would be released then the blade could rotate freely and turn to feather, thus reducing the aerodynamic load. Free rotation of the unclutched blade will increase gradually due to a big moment of inertia, so it is necessary to estimate whether such concept is really effective in terms of fast gust alleviation. In order to address this question a simplified wind turbine model has been built.

Of course, the question arises whether one of existing wind turbine aeroelastic codes could be used, instead of building a new model for calculations. As far as it is known to the authors, such code should be considerably modified, since the wind turbine model which allows free rotation about the blade axis is rather unusual. On the other hand, many wind turbine oriented aeroelastic codes do not even include blade rotational degree of freedom (e.g. BLADED), (Passon et al. 2007) because of high natural frequency corresponding to it. In any case more general aeroelastic codes, not only wind turbine oriented, should be considered. More detailed analysis of aeroelastic codes from the point of view of this paper cannot be done here without detailed knowledge of, and without having access to them.

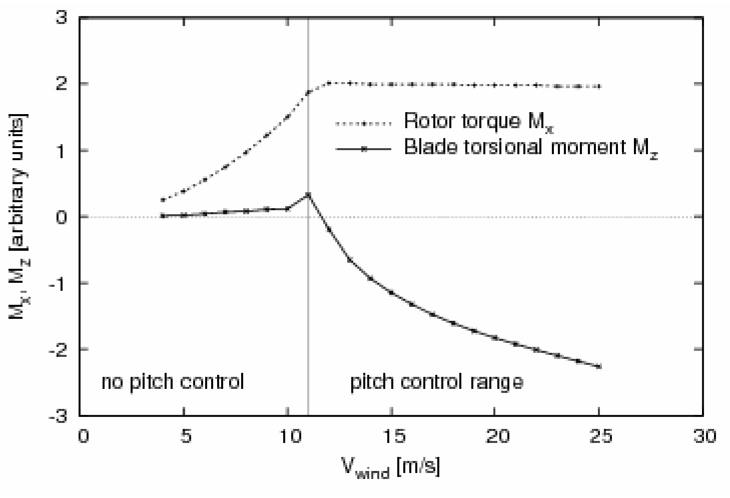


Figure 1. Steady aerodynamic forces.

It should be also emphasized that the aim of this paper is not an engineering background for designing a new device for gust alleviation, but rather presentation of a new idea and numerical verification of its effectiveness.

## 2 SIMPLIFIED WIND TURBINE MODEL

### 2.1 *Assumptions*

The purpose of a simplified wind turbine model is to describe the free motion of a blade after its connection with the hub is unclutched. It is assumed that duration of this process is shorter than a single revolution of the rotor, so all periodic phenomena can be neglected. Further assumptions are as follows:

- The wind turbine rotor is composed of $n_b$ blades ($n_b = 3$).
- The rotor has zero cone and zero tilt angles.
- Each blade is deformable (described by the simple Euler-Bernoulli beam theory) and is connected to the hub with three linear rotational springs.
- The generator is connected to the rotor through the elastic shaft.
- The tower is deformable, however only downwind displacement of the rotor with nacelle and generator is taken into account.
- Quasi-steady aerodynamics within the frame of BEM theory is acceptable.
- All generalized displacements and velocities are small enough for the structural part of equations of motion to be linearized.

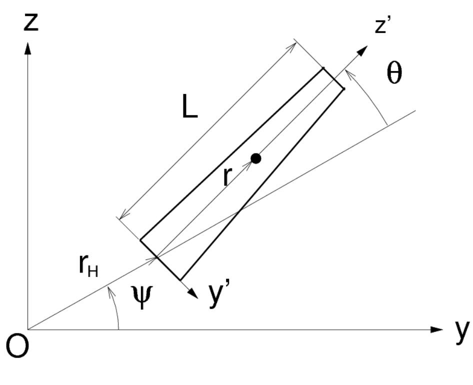


Figure 2. Blade coordinates x'y'z' in a rotor plane Oyz (x and x' axes towards observer).

The sketch of the blade in a rotor plane is shown in Figure 2. The *xyz* is a global coordinate system, while the *x'y'z'* is a blade coordinate system. Each blade is divided into *n* segments along the span ($z'$-axis), and the inertia properties of each blade are modeled by a finite number $n_{mass}$ of concentrated masses (one for each segment), having its own mass, static and inertia moments resulting from given structural properties, distributed along the blade. Each mass has $n_q$ degrees of freedom ($n_q = 3$): $x'$-axis displacement (parallel to $x$-axis) $u$, $y'$-axis displacement $v$, and $z'$-axis rotation $\phi$. There are additional $n_w$ global degrees of freedom ($n_w = 3$): nacelle (tower) downwind displacement $x_T$, rotor and generator rotation angles $\psi$ and $\gamma$, respectively. Finally, the simplified wind turbine model has $n = n_w + n_b \times n_{mass} \times n_q$ degrees of freedom listed in Table 1 (all degrees of freedom that influence the aerodynamic forces are included). For example, for $n_{mass} = 40$, the total number of degrees of freedom equals 363. Degrees of freedom form the vector $\boldsymbol{u}$(t) of generalized coordinates.

Table 1. Wind turbine degrees of freedom (components of vector $\boldsymbol{u}$ (t) of generalized coordinates).

| DOF No | Notation | Description |
|---|---|---|
| 1 | $x_T(t)$ | Nacelle displacement along x-axis (downwind) |
| 2 | $\psi(t)$ | Rotor rotation angle around x-axis |
| 3 (= $n_w$) | $\gamma(t)$ | Generator rotation angle around x-axis |
| ….. | …. | …. |
| $n_w + (k - 1) \cdot n_q + 1$ | $u_k^{(1)}(t)$ | displacement along $x'$-axis of the $k$-th mass of the 1st blade |
| $n_w + (k - 1) \cdot n_q + 2$ | $v_k^{(1)}(t)$ | displacement along $y'$-axis of the $k$-th mass of the 1st blade |
| $n_w + (k - 1) \cdot n_q + 3$ | $\phi_k^{(1)}(t)$ | rotation along $z'$-axis of the $k$-th mass of the 1st blade |
| …. | …. | …. |
| $n_w + n_b + (k - 1) \cdot n_q + 1$ | $u_k^{(2)}(t)$ | displacement along $x'$-axis of the $k$-th mass of the 2nd blade |
| $n_w + n_b + (k - 1) \cdot n_q + 2$ | $v_k^{(2)}(t)$ | displacement along $y'$-axis of the $k$-th mass of the 2nd blade |
| $n_w + n_b + (k - 1) \cdot n_q + 3$ | $\phi_k^{(2)}(t)$ | rotation along $z'$-axis of the $k$-th mass of the 2nd blade |
| …. | …. | …. |
| $n_w + 2 \cdot n_b + (k - 1) \cdot n_q + 1$ | $u_k^{(3)}(t)$ | displacement along $x'$-axis of the $k$-th mass of the 3rd blade |
| $n_w + 2 \cdot n_b + (k - 1) \cdot n_q + 2$ | $v_k^{(3)}(t)$ | displacement along $y'$-axis of the $k$-th mass of the 3rd blade |
| $n_w + 2 \cdot n_b + (k - 1) \cdot n_q + 3$ | $\phi_k^{(3)}(t)$ | rotation along $z'$-axis of the $k$-th mass of the 3rd blade |
| …. | …. | …. |

### 2.2 *Equations of motion*

By using the Lagrange's equations of the second kind the following equations of motion of the wind turbine are obtained:

$$\boldsymbol{M} \cdot \ddot{\boldsymbol{u}} + \boldsymbol{C} \cdot \dot{\boldsymbol{u}} + \boldsymbol{K} \cdot \boldsymbol{u} = \boldsymbol{Q}(\boldsymbol{u}, \dot{\boldsymbol{u}}), \tag{1}$$

where $\boldsymbol{Q}(\boldsymbol{u}, \dot{\boldsymbol{u}})$ is a vector of aerodynamic forces (being nonlinear function of $\boldsymbol{u}$ and $\dot{\boldsymbol{u}}$). Mass $\boldsymbol{M}$, damping $\boldsymbol{C}$ and stiffness $\boldsymbol{K}$ matrices are composed of the following non-zero blocks:

$$\boldsymbol{M} = \begin{bmatrix} \boldsymbol{M}_0 & \boldsymbol{M}_1^{(1)} & \boldsymbol{M}_1^{(2)} & \boldsymbol{M}_1^{(3)} \\ \boldsymbol{M}_1^{(1)T} & \boldsymbol{M}_2^{(1)} & & \\ \boldsymbol{M}_1^{(2)T} & & \boldsymbol{M}_2^{(2)} & \\ \boldsymbol{M}_1^{(3)T} & & & \boldsymbol{M}_2^{(3)} \end{bmatrix}, \boldsymbol{K} = \begin{bmatrix} \boldsymbol{K}_0 & & & \\ & \boldsymbol{K}_2^{(1)} & & \\ & & \boldsymbol{K}_2^{(2)} & \\ & & & \boldsymbol{K}_2^{(3)} \end{bmatrix}, \boldsymbol{C} = \begin{bmatrix} \boldsymbol{C}_0 & & & \\ & \boldsymbol{C}_2^{(1)} & & \\ & & \boldsymbol{C}_2^{(2)} & \\ & & & \boldsymbol{C}_2^{(3)} \end{bmatrix} \tag{2}$$

Mass matrix block components ($i = 1 \ldots n_b$, $k = 1 \ldots n_{mass}$):

$$\boldsymbol{M}_0 = \begin{bmatrix} m_T + m_H + n_b m_B & 0 & 0 \\ 0 & J_H + n_b(J_{zz} + J_{yy} + r_H(m_B r_H + 2S_z)) & 0 \\ 0 & 0 & J_G \end{bmatrix}$$

$$\boldsymbol{M}_1^{(i)} = \begin{bmatrix} \dots & \boldsymbol{M}_{1k}^{(i)} & \dots \end{bmatrix},\ \boldsymbol{M}_{1k}^{(i)} = \begin{bmatrix} m_k^{(i)} & 0 & -S_{yk}^{(i)} \\ 0 & -r_H m_k^{(i)} - S_{zk}^{(i)} & -r_H S_{xk}^{(i)} - J_{zxk}^{(i)} \\ 0 & 0 & 0 \end{bmatrix}$$

$$\boldsymbol{M}_2^{(i)} = \begin{bmatrix} \ddots & & \\ & \boldsymbol{M}_{2k}^{(i)} & \\ & & \ddots \end{bmatrix},\ \boldsymbol{M}_{2k}^{(i)} = \begin{bmatrix} m_k^{(i)} & 0 & -S_{yk}^{(i)} \\ 0 & m_k^{(i)} & S_{xk}^{(i)} \\ -S_{yk}^{(i)} & S_{xk}^{(i)} & J_{sk}^{(i)} \end{bmatrix} \tag{3}$$

The blade inertia parameters are defined as follows (note that this notation differs from commonly used in text books, but is more convenient while programming):

$$m_k{}^{(i)} = \int dm,\quad S_{xk}{}^{(i)} = \int x'dm,\quad S_{yk}{}^{(i)} = \int y'dm,\quad S_{zk}{}^{(i)} = \int z'dm$$

$$J_{yyk}{}^{(i)} = \int y'^2 dm,\ J_{zxk}{}^{(i)} = \int z'x'dm,\ J_{zzk}{}^{(i)} = \int z'^2 dm,\ J_{sk}{}^{(i)} = \int \left(x'^2 + y'^2\right) dm \tag{4}$$

where integration is carried out over the k-th segment of the i-th blade. Stiffness matrix non-zero block components:

$$\boldsymbol{K}_0 = \begin{bmatrix} k_T & 0 & 0 \\ 0 & k_G & -k_G \\ 0 & -k_G & k_G \end{bmatrix}, \tag{5}$$

$$\boldsymbol{K}_2^{(i)} = \boldsymbol{U}^{(i)^{-1}}. \tag{6}$$

where $\mathbf{K}_2{}^{(i)}$ is the matrix of stiffness influence coefficients of the flexible blade while $\mathbf{U}^{(i)}$ is the corresponding matrix of flexibility influence coefficients which can be calculated according to e.g. (Bisplinghoff 1955).

Damping matrix elements are assumed proportional to the stiffness matrix elements. A good validation of the presented model is solution to the eigenvalue problem

$$\omega^2 \cdot \boldsymbol{M} \cdot \boldsymbol{u}_0 = \boldsymbol{K} \cdot \boldsymbol{u}_0. \tag{7}$$

The most significant eigenvalues compared to the BLADMODE (Lindenburg 2003) results (Van Langen 20007) are given in Table 2.

Table 2. Natural frequencies.

| Description | BLADMODE (Hz) | Present method (Hz) | Rel. difference (%) |
|---|---|---|---|
| Reaction-less: | | | |
| 1st flap | 0.6386 | 0.6569 | 2.9 |
| 1st edge | 1.0885 | 1.0917 | 0.3 |
| 2nd flap | 1.8632 | 1.9059 | 2.3 |
| 2nd edge | 3.9309 | 3.9614 | 0.8 |
| Torsion | 5.3267 | 5.4789 | 2.9 |
| Collective: | | | |
| Tower | 0.3176 | 0.3185 | 0.3 |
| 1st flap | 0.6576 | 0.6750 | 2.6 |
| 1st edge | 1.7266 | 1.7149 | -0.7 |
| 2nd flap | 1.8873 | 1.9295 | 2.2 |
| 2nd edge | 2.9973 | 2.9977 | 0.01 |
| Torsion | 5.3219 | 5.4732 | 2.8 |

The results of the present method correspond to forty concentrated masses per blade. It can be seen that the present method gives in general slightly higher values than the BLADMODE code, but overall discrepancy does not exceed 3%. The lowest eigenvalue of Equation 7 is equal to zero because of the possibility of free rotation of the rotor as a rigid body, and is a consequence of the structure of $\boldsymbol{K}_0$ matrix (Eq. 5).

Second order Equation 1 can be transformed to the first order equation in a standard way by introducing vector $\boldsymbol{q}$ of new coordinates:

$$\boldsymbol{q} = \begin{Bmatrix} \boldsymbol{u} \\ \dot{\boldsymbol{u}} \end{Bmatrix}, \tag{8}$$

which gives the following first order equation of motion:

$$\dot{\boldsymbol{q}} = \begin{bmatrix} \boldsymbol{0} & \boldsymbol{I} \\ -\boldsymbol{M}^{-1}\cdot\boldsymbol{K} & -\boldsymbol{M}^{-1}\cdot\boldsymbol{C} \end{bmatrix}\boldsymbol{q} + \begin{Bmatrix} \boldsymbol{0} \\ \boldsymbol{M}^{-1}\cdot\boldsymbol{Q}(\boldsymbol{q}) \end{Bmatrix} \tag{9}$$

## 2.3 *Aerodynamic forces*

Aerodynamic forces were calculated by using the blade element momentum theory, described for example by (Hansen 2008) or (Burton et al. 2006). According to this theory, aerodynamic forces are calculated separately in each two-dimensional section of the blade, perpendicular to the span, based on wind tunnel data, and then are integrated along the blade span. Thus each component $Q_i$ ($i$= 1... $n$) of the vector **Q** is of the form:

$$Q_i = \sum \int_0^L F_i(r)dr \tag{10}$$

where $F_i$ *(r)* is the generalized force per unit span corresponding to the $i$-th generalized coordinate and the sum covers all three rotor blades. For instance, for $i = 1$ (rotor thrust)

$$F_i(r) = \frac{\rho(W(r))^2}{2} C_n(r)c(r) \tag{11}$$

where *W(r)* is the magnitude of wind velocity relative to the blade section, *c(r)* is the blade chord, and $C_n(r)$ is the lift coefficient normal to the rotor plane (ρ is the air density). Both the magnitude of the velocity and the angle of attack it forms with the chord direction are iteratively calculated according to the blade element momentum theory (Hansen 2008). Having all terms in Equation 9 determined, the equation can be integrated numerically by using e.g. Runge-Kutta method.

Regardless of the method of solving Equation 1 one condition must be satisfied. The torsional moment $M_z$ twisting blade at root should be negative in a certain neighborhood of the reference steady motion. In the paper, such motion has been assumed at $V_{Wind}$ = 24 m/s. To validate results of aerodynamic moment calculation, a comparison with the BLADMODE code has been made for 20 deg pitch angle (Van Langen 2007), shown in Figures 3a and 3b. Although the blade tip displacements differ rather significantly, the overall agreement in the Mz moment is good. Note that the BLADMODE code uses the non-slender beam theory with large deflections and more sophisticated aerodynamic theory.

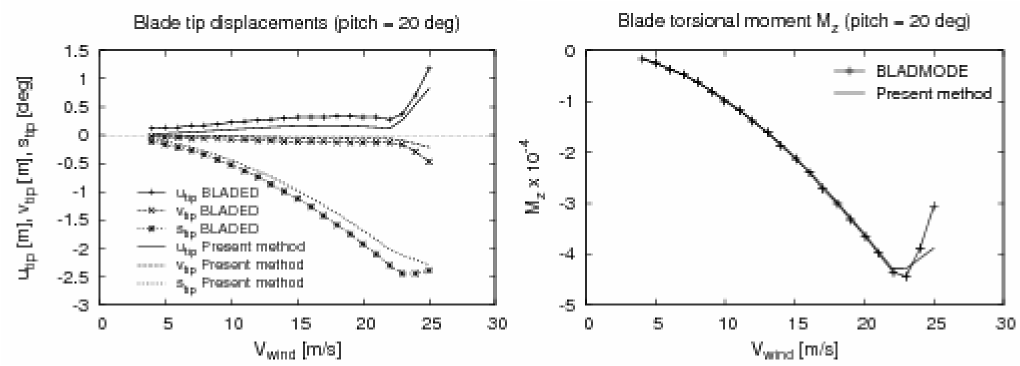


a) b)

Figure 3. Comparison with BLADMODE: a) Tip deformations, b) Torsional moment at root.

## 3 STANDARD MAGNIFIED GUST RESPONSE

As a sample gust profile a standard gust profile has been taken, according to (IEC 2005), with the peak value magnified approximately three times, shown in Figure 4a.

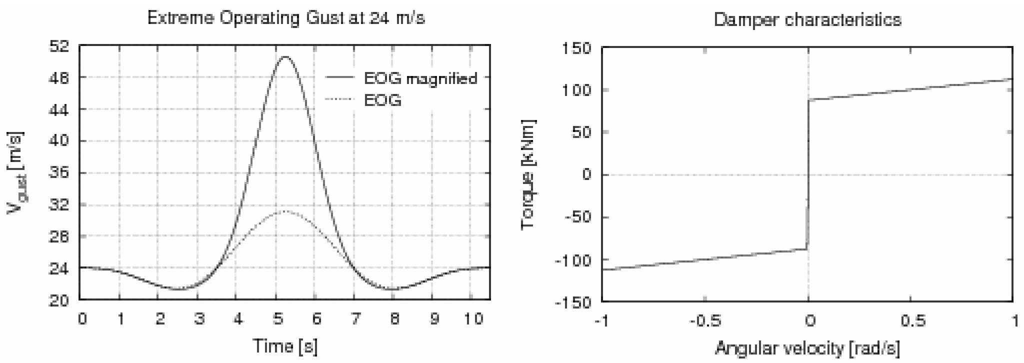


a) b)

Figure 4. a) Standard and magnified gust profiles b)Damper characteristics.

Such a gust causes a significant change in aerodynamic forces, shown in Figure 5b. It is worth-noting, that two aerodynamic moments generated by gust, $M_x$ and $M_y$, follow the gust profile. The exception is the blade torsional moment $M_z$, absolute value of which increases as the gust decays, and decreases as the gust grows. The torsional moment is negative, but reaches small positive values in the neighborhood of peak values of the gust. It means that the blade is forced to turn to feather if the gust velocity is not too high. The blade out of plane bending moment $M_y$ caused by gust is shown in Figure 6. Its peak value is approximately one order of magnitude greater than the nominal value.

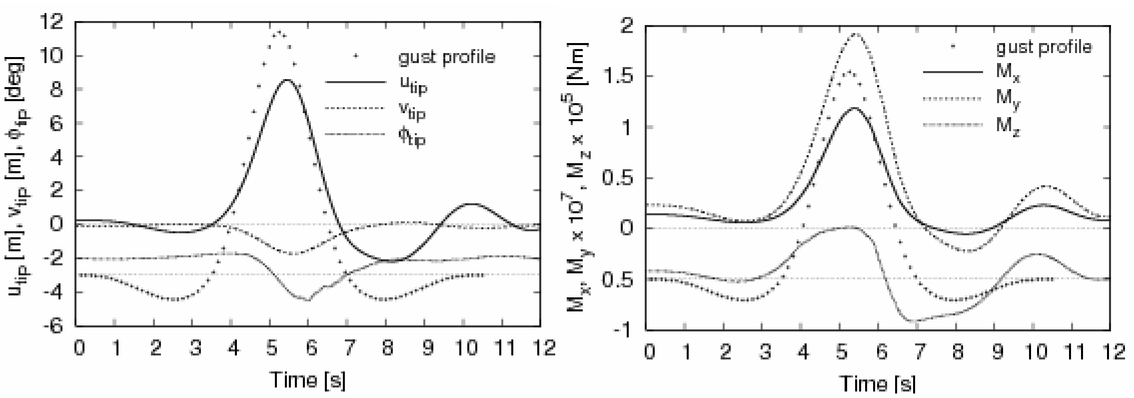


a) b)

Figure 5. Gust response: a) Tip deformations, b) Aerodynamic moments in the blade root.

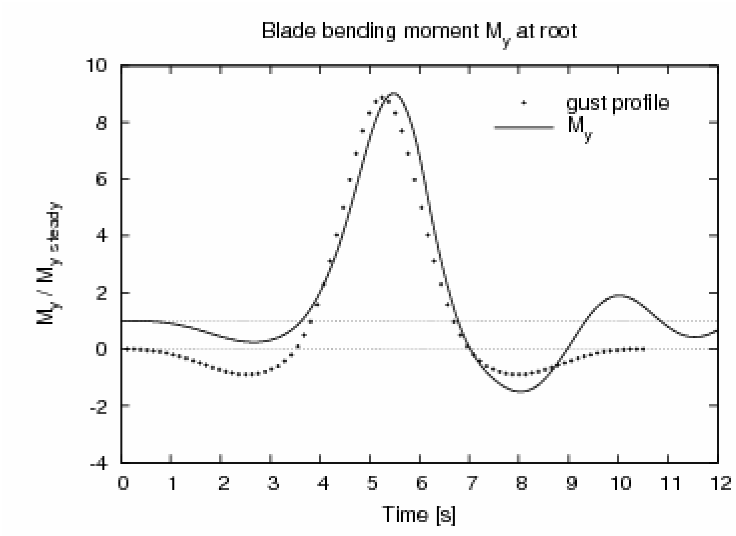


Figure 6. Non-dimensional gust response.

## 4 BLADE UNCLUTCHING AND CLUTCHING-BACK SIMULATION

### 4.1 *Adaptation strategy*

The numerical simulation describes the blade motion upon the gust detection (phase 1 in Fig. 7) and settinng the rotation of a blade free. The unclutching process takes 0.05 s. In numerical simulation it means, that during this short interval the torsional stiffness of blade-hub connection drops to zero. Just after unclutching, the blade rotation angle (being really an actual pitch angle with opposite sign) decreases very fast (phase 2 in Fig. 7) and reaches a given threshold value (10 degrees in the simulation). After that, the braking process starts (phase 3 in Fig. 7) and continues until the angular velocity of the blade reaches zero. It has been assumed that the braking moment characteristic at a blade root is as shown in Figure 4b.

Then the process of coupling back the blade and the hub takes place. These parts should be connected together while their relative velocity is equal to zero in order to avoid a harmful impact. In general, the clutch should be a mechanical device placed on top of the pitch control mechanism, and under normal operating conditions should not affect the work of the turbine. After the blade is connected to the hub, the initial state is restored (phase 4 in Fig. 7) by using the existing pitch control mechanism.

### 4.2 *Results*

The effect of simulation in terms of the out-of-plane blade bending moment *My* is shown in Figure 8. It can be seen that the peak value has been reduced by 65%, compared to 55% obtained with the simulated 7 deg/s pitch rate control mechanism.

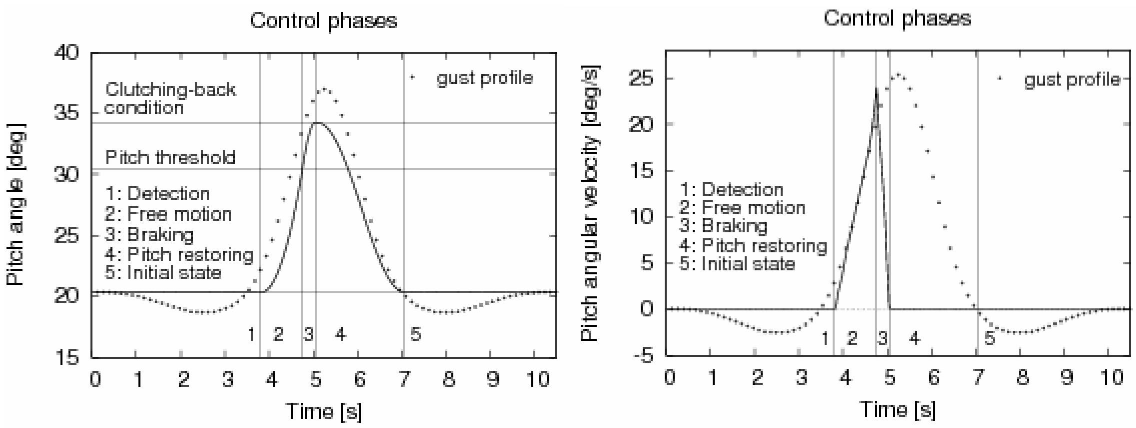


a) b)

Figure 7. Control phases of blade unclutching: a) Pitch angle b) Pitch angular velocity

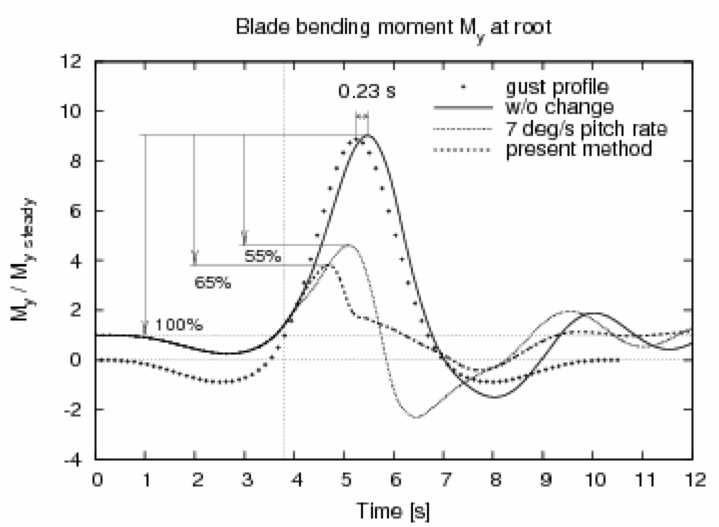


Figure 8. Gust load reduction - final result.

# 5 MODAL METHOD

## 5.1 *Introduction*

Direct integration of the equations of motion is inefficient in terms of machine computation time. Un-clutching and clutching back are transient processess and require a small integration step, resulting in even longer computation time. Therefore an attempt has been made to solve the problem formulated in previous chapters using the modal method. For this purpose two sets of eigenmodes and eigenfrequencies have been calculated, one corresponding to fixed blade-hub connection and one allowing for free rotation about the blade axis. In the latter case two rigid mode shapes have been obtained, i.e. rotor revolution and blade rotation about its main axis. The key feature of the adaptation process involved here is switching between the two sets of eigenmodes, depending if the balde is being unclutched or clutched back.

## 5.2 *Problem formulation*

The wind turbine model has *n* degrees of freedom in generalized coordinates, cf. Table 1. Vector **q** may be expressed in terms of modal coordinates **y** as $\boldsymbol{q} = \boldsymbol{W} \cdot \boldsymbol{y}$, where columns of **W** are the eigenvectors. The dimension of the problem is then reduced from *n* to *k* if *k* eigenmodes are considered. Eigenmodes obtained from the eigenvalue problem can be divided into three groups, i. e. rigid, reaction-less and collective. Rigid ones refer to rotor revolution and unclutched blade rotation. Reaction-less are the modes in which the tower motion is constrained, and collective ones, which are symmetric, refer to the whole turbine motion. It can be observed that only rigid and collective modes participate in the real motion and thus need to be included in the analysis. For the turbine under consideration there are fourteen collective mode shapes out of first forty taken into account. As a result the dimension of the task is reduced from 363 (if 40 masses per blade are taken) to 15 (1 rigid+ 14 collective modes). The error resulting from neglecting *n-k* modeshapes is insignificant.

For the present problem torsional motion is of utmost importace, hence three torsional mode shapes were considered, even though in some commercial codes, f.e. BLADEMODE no torsional d.o.f. are included, which is acceptable for most analyses.

The equations of motion in modal coordinates are as follows:

$$\begin{Bmatrix} \ddot{y}_1 \\ .. \\ \ddot{y}_n \end{Bmatrix} + \begin{Bmatrix} \dfrac{c_1}{\mu_1} y_1 \\ .. \\ \dfrac{c_n}{\mu_n} y_n \end{Bmatrix} + \begin{Bmatrix} \omega_1^2 y_1 \\ .. \\ \omega_n^2 y_n \end{Bmatrix} = \begin{Bmatrix} \mu_1^{-1} \boldsymbol{w}_1^T \boldsymbol{Q}(\boldsymbol{W} \cdot \boldsymbol{y}) \\ .. \\ \mu_n^{-1} \boldsymbol{w}_n^T \boldsymbol{Q}(\boldsymbol{W} \cdot \boldsymbol{y}) \end{Bmatrix} \tag{12}$$

where **Q** is the aerodynamic forces vector, $\omega_i$ are the eigenfrequencies, $c_i$ are the damping coefficients, and $\mu_i$ are generalized masses. Damping coefficients are related to the fractions of critical damping of *i*-th mode $\xi_i$ as shown on Equation 13:

$$\frac{c_i}{\mu_i} = 2 \cdot \xi_i \cdot \omega_i \tag{13}$$

Generalized masses are defined as $\mu_i = \boldsymbol{w}_i^T \cdot \boldsymbol{M} \cdot \boldsymbol{w}_i$, where $\boldsymbol{M}$ is the mass matrix and $\boldsymbol{w}_i$ are columns of the $\boldsymbol{W}$ matrix. If $\boldsymbol{w}_i$ are normalized with respect to $\boldsymbol{M}$ then all generalized masses are equal to 1.0: $\boldsymbol{W}^T \cdot \boldsymbol{M} \cdot \boldsymbol{W} = \boldsymbol{I}$, and the following relationship holds:

$$\boldsymbol{W}^T \cdot \boldsymbol{K} \cdot \boldsymbol{W} = \begin{bmatrix} \omega^2{}_1 & & \\ & .. & \\ & & \omega^2{}_n \end{bmatrix} \tag{14}$$

Finally, after transferring the system from second to first order equations, the following set of equations is obtained:

$$\dot{\boldsymbol{Y}} = \begin{Bmatrix} \boldsymbol{0} \\ \boldsymbol{F}_{MOD}(\boldsymbol{y}) \end{Bmatrix} + \begin{bmatrix} \boldsymbol{0} & \boldsymbol{I} \\ -\boldsymbol{\Omega} & -\boldsymbol{C} \end{bmatrix} \cdot \boldsymbol{Y}, \quad \dot{\boldsymbol{Y}} = \begin{Bmatrix} \dot{\boldsymbol{y}} \\ \ddot{\boldsymbol{y}} \end{Bmatrix}, \quad \boldsymbol{Y} = \begin{Bmatrix} \boldsymbol{y} \\ \dot{\boldsymbol{y}} \end{Bmatrix} \tag{15}$$

, where:

$$\boldsymbol{F}_{MOD}(\boldsymbol{y}) = \begin{Bmatrix} \boldsymbol{w}_1^T \cdot \boldsymbol{Q}(\boldsymbol{W} \cdot \boldsymbol{y}) \\ .. \\ \boldsymbol{w}_n^T \cdot \boldsymbol{Q}(\boldsymbol{W} \cdot \boldsymbol{y}) \end{Bmatrix}, \boldsymbol{\Omega} = \begin{bmatrix} \omega_1^2 & & \\ & .. & \\ & & \omega_n^2 \end{bmatrix}, \boldsymbol{C} = \begin{bmatrix} 2 \cdot \xi_1 \cdot \omega_1 & & \\ & .. & \\ & & 2 \cdot \xi_n \cdot \omega_n \end{bmatrix} \tag{16}$$

Each element $F_{MOD,i}$ of the vector of generalized forces $\boldsymbol{F_{MOD}}$ is the work done by external forces on *i*-th mode without contribution of all remaining modes. In aeroelastic problems right-hand side vector is solution dependent. Hence, the system cannot be separated into *k* independent equations of simple oscillators, which is a common technique in many modal method applications. Vector $\boldsymbol{F}$ can be further expressed as:

$$F_{MOD,i} = F_{ax} \cdot w_{1,i} + M_{aero} \cdot w_{2,i} + (-1) \cdot M_{torque} \cdot w_{3,i} + \sum_{j=1}^{n_{mass}} FC^{ss}{}_j \cdot w^{ss}{}_j, \; i = 1..k \tag{17}$$

where

$$FC^{ss}{}_j = \int_{r\_1}^{r\_2} Q^{ss}(\boldsymbol{q},t)dr, \quad ss = u,v,s \tag{18}$$

First three terms in Equation 17 include forces corresponding to global degrees of freedom, i.e. total axial force, total aerodynamic moment about the turbine axis and the generator torgue. Under the sum there is a product of appropriate aerodynamic, concentrated force integrated over a section of a blade between radius coordinates *r_1* and *r_2,* and the corresponding element of the mode shape vector. Parameters *u, v, s* refer to flap-wise, edge-wise and torsional d.o.f. respectively and $n_{mass}$ is the number of concentrated masses.

### 5.3 *Adaptation process*

The adaptation strategy has already been discussed in Paragraph 4. The implementation of this strategy with use of modal method is discussed in this section.

At the time instant $t_0$ the blade is unclutched, hence the solution at $t_0$-$\Delta t$ is $\boldsymbol{q}^A = \boldsymbol{W}^A \cdot \boldsymbol{y}^A$, whereas the solution at $t_0$ and subsequent time instants is $\boldsymbol{q}^B = \boldsymbol{W}^B \cdot \boldsymbol{y}^B$. $\boldsymbol{W}^A$ and $\boldsymbol{W}^B$ are sets of eigenmodes with fixed and freed blade rotation, respectively. Vector $\boldsymbol{y}_B$ needs to be found, such that the difference between $\boldsymbol{q}^A$ and $\boldsymbol{q}^B$ is minimized. The number of equations is $n$ whereas the number of unknowns is $k$. The problem may be defined as follows: find $\boldsymbol{y}_B$, such that

$$f(\boldsymbol{y}_B) = \sum_{j=1}^{n} e_j^{\,2}, \quad e_j = \sum_{i=1}^{k} (w^B_{j,i} \cdot y^B_i - w^A_{j,i} \cdot y^A_i) \tag{19}$$

is minimized. This can be solved using various optimization techniques, f.e. gradient optimization of a function with $k$ arguments.

A similar problem is encountered when the blade is clutched back. The total error $f$ of transition between two sets of mode shapes is 0.06 % for unclutching and 0.4% for clutching back. The distribution of the error of transition between two sets of eigenmodes along a blade is shown in Figure 9.

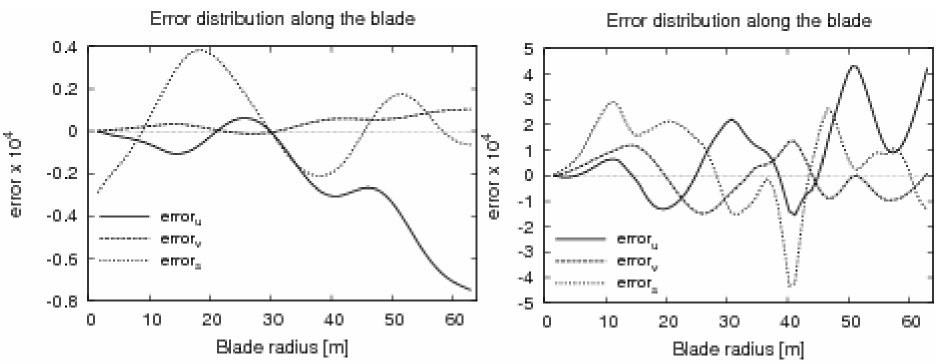


a) b)

Figure 9. Error distribution along the blade: a) unclutching b) clutching back.

After calculating the vector of modal coordinates $\boldsymbol{y}$ in a fast and efficient way, the phisical cooradinates can be obtained and eventually dynamical reactions at the blade root may be also calculated.

## 6 CONCLUSIONS

Based on the results of numerical simulations the following conclusions can be drawn:

– It is possible to reduce aerodynamic loads acting on a wind turbine in a short time by releasing the blade-hub connection (blade unclutching) and controlling this process in response to a sudden gust, and also under normal operating conditions (when blade rotational moment is negative).

– The proposed response is faster than obtained for pitch rates offered by regular pitch control mechanisms.

Further, the proper control algorithm should be implemented.

The authors realize that the presented concept is only an idea and before its eventual materialization a lot of engineering work has to be done, results of which may be not encouraging.

## ACKNOWLEDGMENT

The financial support from the projects “Smart Technologies for Safety Engineering – SMART and SAFE” – TEAM Programme – granted by the Foundation for Polish Science and “Health Monitoring and Lifetime Assessment of Structures” – MONIT – POIG.01.01.02-00-013/08-00 from the EU Structural Funds in Poland is gratefully acknowledged.

## APPENDIX: NOMENCLATURE (NOT DESCRIBED PREVIOUSLY IN THE PAPER)

$r_H$ hub radius (Fig. 2)
$m_T$ blade mass
$m_H$ hub mass
$m_T$ equivalent mass of tower with nacelle with respect to the displacement along x-axis
$S_x$ blade mass first moment of inertia with respect to the y'z'-plane
$S_y$ blade mass first moment of inertia with respect to the x'z'-plane
$S_z$ blade mass first moment of inertia with respect to the x'y'-plane (root)
$J_H$ hub mass second moment of inertia with respect to the x-axis
$J_{xx}$ blade mass second moment of inertia with respect to the y'z'-plane
$J_{yy}$ blade mass second moment of inertia with respect to the x'z'-plane
$k_T$ tower+nacelle fore-aft bending equivalent spring stiffness
$k_G$ rotor-generator shaft torsional stiffness

## REFERENCES

Bisplinghoff R.L., Ashley H., Halfman R.L. 1955. *Aeroelasticity.* Cambridge: Addison-Wesley Publishing Co.

Burton T, Sharpe D, Jenkins N, Bossanyi E .2006. *Wind energy handbook*. New York: John Wiley.

Hansen M.O.L. 2008. *Aerodynamics of Wind Turbines.* London: Earthscan

Lindenburg C. 2002. Aeroelastic modeling of the LMH64-5 blade. *DOWEC-083\ECN-C-03-020*. Petten, ECN.

Lindenburg C. 2003. BLADMODE, Program for Rotor Blade Mode Analysis. *ECN-C-2-050*. Petten, ECN.

Passon P., Kuhn M., Butterfield S., Jonkman J., Camp T., Larsen T.J. 2007. OC3-Benchmark Exercise of Aero-elastic Offshore Wind Turbine Codes. *Conference Paper NREL/CP-500-41930*.

Van Langen, P.J. 2007. Aeroleastic Analysis of the UpWind reference wind turbine (Draft*). ECN-E-07-000*. ECN.

IEC. *Wind turbines—Part 1: Design requirements.* IEC 61400-1, 2005 (Third Edition).